Atherosclerosis 403 (2025) 119130

Contents lists available at ScienceDirect

Atherosclerosis

journal homepage: www.elsevier.com/locate/atherosclerosis

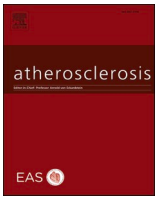

Advancing atherosclerosis research: The Power of lipid imaging with MALDI-MSI

Christoph H.M. Bookmeyer [a,b,*], F. Xavier Correig [a,b,c], Luis Masana [b,c,d], Paolo Magni [e,f], Óscar Yanes [a,b,c], Maria Vinaixa [a,b,c,**]

[a] Universitat Rovira i Virgili, Department of Electronic Engineering, Metabolomics Interdisciplinary Laboratory, Tarragona, Spain
[b] CIBER de Diabetes y Enfermedades Metabólicas Asociadas, Instituto de Salud Carlos III, Spain
[c] Institut d'Investigació Sanitària Pere Virgili (IISPV), Tarragona, Spain
[d] Universitat Rovira i Virgili, Research Unit on Lipids and Atherosclerosis, Reus, Spain
[e] Dept. of Pharmacological and Biomolecular Sciences, Università degli Studi di Milano, Milan, Italy
[f] IRCCS MultiMedica, Sesto S. Giovanni, Italy

ARTICLE INFO

Keywords:
Atherosclerosis
MALDI-MSI
Mass spectrometry imaging
Lipids
Spatial lipidomics

ABSTRACT

Atherosclerosis is a chronic inflammatory disease that is one of the leading causes of mortality globally. It is characterized by the formation of atheromatous plaques in the intima layer of larger arteries. The (fibro-)fatty plaques usually develop asymptomatically within the vessel until a serious event such as myocardial infarction or stroke occurs. Lipids play a pivotal role in disease progression, but while the causal role of cholesterol is beyond doubt, the distribution of numerous other lipids within the heterogeneous layers of atherosclerotic plaques, and their biological function remain unclear. A deeper understanding of the pathophysiological progression of the disease for prognostics, diagnostics, treatment, and prevention is of great need. Mass spectrometry imaging (MSI), in particular with matrix-assisted laser desorption/ionization (MALDI) offers an unprecedented untargeted characterization of the physiological microenvironment, unraveling the spatial distribution of numerous biochemical compounds. MALDI-MSI offers an advantageous balance of sample preparation, chemical sensitivity, and spatial resolution, and thus has been established as a key technology in modern biomedical analysis. This review focuses on the analysis of lipids in atherosclerotic lesions with MALDI-MSI, for which the past years showed major developments in the spatial characterization of lipids and their interaction within atherosclerotic plaques. We will cover main contributions with a focus on the recent decade, elaborate possibilities, limitations, main findings, and recent developments from sample handling to instrumentation, and estimate current challenges and potentials of MALDI-MSI with respect to a clinical application.

1. Atherosclerosis

Atherosclerosis is the underlying mechanism of several cardiovascular diseases (CVDs) and has been described in detail in recent overview articles [1]. More than 80 % of fatal CVDs are caused by coronary heart disease or ischemic stroke. Atherosclerosis comprises a complex scenario with numerous factors contributing to the development of severe complications, based on heterogeneous deposits of lipids and necrotic debris within the artery, which often remain unnoticed for decades.

The development of plaques begins with an accumulation of cholesterol in the artery wall mainly due to low-density lipoprotein penetrating from the bloodstream through the endothelial layer, leading to an inflammatory response in the vascular wall [2,3]. The consequent aggregation of large amounts of cholesterol and further lipids in the intima attracts monocytes from the bloodstream. These transform into macrophages, internalize the accumulated lipoproteins, and eventually engorge to become foam cells [4]. Ultimately, the death of these foam cells releases their lipid-laden contents, forming a lipo-necrotic core. This sustains inflammation, promoting vascular smooth muscle cells (VSMCs) to migrate from the media layer, synthesize the extracellular matrix, and encapsulate the lesion with a protective fibrous cap. With

* Corresponding author. Universitat Rovira i Virgili, Department of Electronic Engineering, Metabolomics Interdisciplinary Laboratory, Tarragona, Spain.
** Corresponding author. Universitat Rovira i Virgili, Department of Electronic Engineering, Metabolomics Interdisciplinary Laboratory, Tarragona, Spain.
E-mail addresses: Christoph.bookmeyer@urv.cat (C.H.M. Bookmeyer), maria.vinaixa@urv.cat (M. Vinaixa).

https://doi.org/10.1016/j.atherosclerosis.2025.119130
Received 15 September 2024; Received in revised form 1 December 2024; Accepted 4 February 2025
Available online 15 February 2025

further cell death and lipid release, a large lipid core grows.

The major threat of atherosclerosis is the rupture of the encapsulating fibrous cap, which releases large amounts of lipids into the bloodstream, triggering the formation of thrombi with severe clinical consequences. The vulnerability or stability of plaques is determined rather by their chemical composition than their size, influenced by impairments in metabolism, micronutrient distribution, and cellular exchange [1]. An atherosclerotic lesion constitutes seven distinct regions: outer VSMCs, inner VSMCs, collagen-rich area, hemorrhage, calcification, macrophage-rich area, and lipid-necrotic core (Fig. 1).

Several factors in the heterogeneous cellular setup contribute to the plaque's rupture, i.e., the senescence of VSMCs or macrophages, microcalcification, lipid accumulation, inflammatory composition, or necrosis [1]. However, the underlying spatio-temporal processes remain largely unknown. Molecular investigations are urgently needed to capture intrinsic tissue and plaque heterogeneity. In this context, sophisticated molecular imaging techniques such as MALDI-MSI can reveal momentous insights into these unresolved questions [7]. The spatial characterization of the lipidome can majorly enhance the understanding of lipid dysregulation and key factors contributing to plaque progression [8].

2. MALDI-MS imaging

Mass spectrometry imaging (MSI) is a label-free imaging technique that allows for the simultaneous detection of hundreds of molecules and their spatial distribution in biological tissue sections. MALDI is the most prevalent ionization approach for biomedical MSI, being widely adopted in laboratories globally. The technique offers relatively comprehensive molecular coverage of complex biological samples, allowing for the determination of specific molecular roles and simultaneous regulatory processes at tissue level. For heterogeneous tissues, the morphological information and high spatial integrity enhance the analytical depth, as tissue types in close proximity have distinct chemical compositions. The most prominent ion source MALDI employs a laser that rasters a thin tissue section covered with an organic matrix. This matrix effectively translates the laser energy to the biomolecules and aids the transition of analyte ions into the gas phase. The range of accessible analytes depends on several technical parameters, such as the matrix composition and the technique applied to deposit it onto the tissue section, polarity, ion source design as also the downstream mass spectrometer (see below). However, MALDI does not require detailed previous knowledge of the analytes of interest – it can therefore be deemed "untargeted". It can identify diagnostic and prognostic biomarkers and elucidate significant contributors to the underlying metabolic mechanisms directly *in situ*, often before the occurrence of symptoms. With these merits, MALDI-MSI has contributed to an ever-growing number of biochemical and clinical analyses in the past decades with unmatched detail. Comprehensive reviews about MALDI-MSI, the challenges in biochemical imaging, and the opportunities in clinical application and translational medicine have recently been published [9,10].

MSI has gained interest in unraveling the mechanisms of CVD and atherosclerosis. Initial studies used secondary ion mass spectrometry (SIMS) [11], but soon, the advantages of MALDI-MSI yielding a lower degree of fragmentation and improved sensitivity and molecular coverage compared with SIMS [9,12,13] were recognized – a review article described these early MSI analyses of atherosclerosis identifying contributors to its progression [14]. Mezger et al. provided an overview of protein/peptide, lipid, and metabolite analysis in CVD, highlighting trends in these complementary MSI approaches [7]. Additionally, a recent comment introduced key publications using MALDI-MSI [15].

Due to the crucial role of lipids in the initiation and progression of atherosclerotic plaques, an increasing number of studies focused on investigating the atherosclerotic lipidome with MALDI-MSI in the recent decade. Advances in the MALDI-MSI field enabled researchers to unravel specific contributions of lipids and metabolites in the affected tissue. They demonstrated the potential of MALDI-MSI for clinical applications by identifying co-localizations of lipid profiles with distinct plaque subregions in different stages of disease progression. This review therefore focuses on MALDI-MSI for analysis of the atherosclerotic lipidome, comparing the recent complex findings in greater detail. We summarize technical advances, optimized protocols, identified universal bioindicators, their biological and pathological relevance, and the steps towards establishing MALDI-MSI lipidomics for clinical routine.

2.1. Experimental workflow of MALDI-MSI

Fig. 2 illustrates the general workflow of a MALDI-MSI experiment, which comprises the three main parts sample preparation, MSI acquisition, and Data Processing & Visualization. Each experimental step must preserve spatial integrity to ensure comparability between measurements. Sample preparation – akin to classical histology techniques – involves the optional embedding of the tissue in a medium (depending on the tissue's shape), cryosectioning of the frozen biological tissue at usually 5–15 μm, and mounting the thin sections on suitable slides. Researchers working with small organ structures like atheromas often use embedding media like gelatine, agarose, or derivates of celluloses, as they produce only minute MALDI background signals, as opposed to OCT (optimal cutting temperature) compound.

Fixation, commonly used to prevent morphological alteration in classical histology, is typically avoided in MALDI-MSI, as agents like formalin-fixed paraffin embedding (FFPE) chemically alter the tissue by covalently cross-linking compounds [9]. For general lipidomics, no treatment such as washing or deparaffinization is necessary, as lipids often produce strong signals from native tissue [16].

In the next step, a matrix adapted to the MALDI process is applied. This is usually performed with an automated sprayer or via sublimation, aiming for a homogeneous thin layer with small matrix crystal sizes in the order of micrometers that ensures a consistent response in the LDI process [9]. Then, a laser is focused with precise energy on the tissue

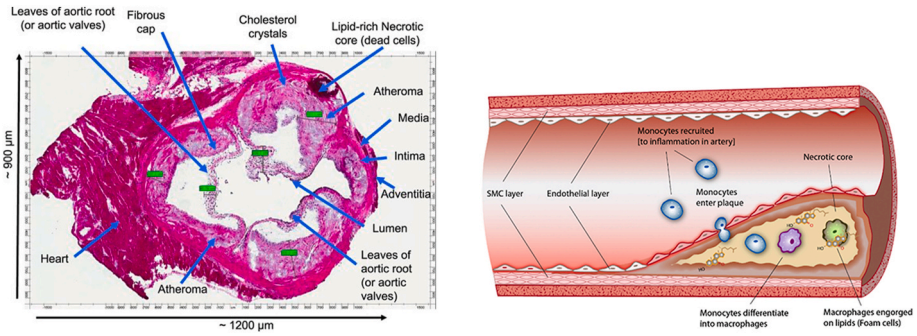

Fig. 1. Left: H&E-stained aorta from ApoE KO mouse showing different lesion regions and histomorphology - from Ref. [5], right: Formation of foam cells and arterial plaque – from Ref. [6] ©Wiley; Elsevier.

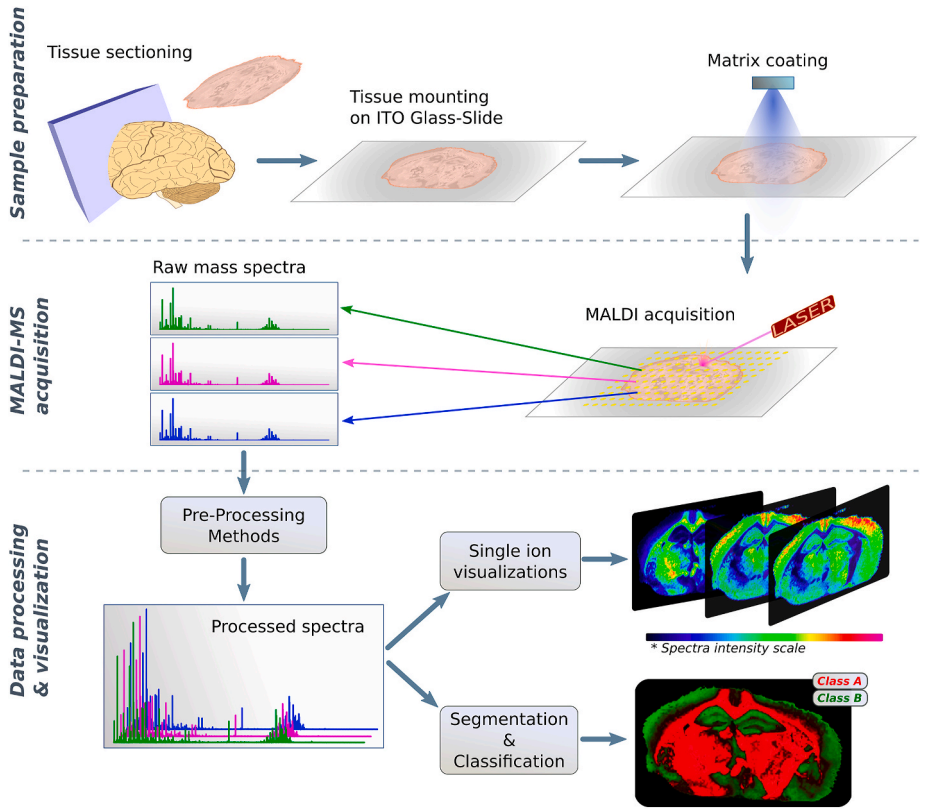

Fig. 2. Typical workflow of a MALDI-MSI experiment [17]. ©PLOS ONE.

section to initiate the "soft" desorption and ionization of compounds: The organic matrix absorbs the incorporated laser energy, protecting the biochemical analytes from direct irradiation, converting the laser energy to these compounds, and supporting the explosive ablation into the gas phase. This concerted process yields mostly singly charged ions of polar to mid-polar compounds with minimal analyte fragmentation. When sampling the tissue with the laser in a spatially controlled raster, the defined molecular profiles can be reconstructed into a histopathological image.

The matrix's ionization properties determine which analytes can be detected, particularly considering polarity. Proton transfer reaction and adduct formation with ions like Na^+, K^+ or OAc^- are the predominant mechanisms of ionization. For lipid analysis, 2,5-dihydroxybenzoic acid (DHB) and α-cyano-4-hydroxycinnamic acid (CHCA) are commonly used matrices for the (+)-ion mode, and 9-aminoacridine (9AA) and 2,6-dihydroxyacetophenone (DHA) in the (−)-ion mode. More recently 1,5-diaminonaphthalene (DAN) was introduced for dual-polarity [7].

The expected lipid classes in the MALDI-MSI (+)-ion mode include phosphatidylcholines (PC), sterols (ST) including cholesterol and cholesteryl esters (CE), sphingomyelins (SM), cerebrosides, and di-/triacylglycerols (DAG/TAG). In the (−)-ion mode, phosphatidylethanolamines (PE), phosphatidylserines (PS), phosphatidylinositols (PI), phosphatidylglycerols (PG), further sphingolipid classes, cardiolipins (CL), and STs can be detected [16,18,19].

In section 4, we will point out lipids specific to atherosclerosis and in section 5, we will discuss challenges in simultaneously detecting these vast numbers of compounds, such as ion suppression effects and near-isobaric signals.

The complex data generated in MALDI-MSI requires sophisticated data processing for compound identification. This complexity arises from: a) the simultaneous generation of multiple ions without chromatographic separation, including corresponding isotopes, adducts, and in-source fragmentation products; b) unpredictable ionization yields; c) sample preparation inhomogeneities; and d) technical bias in the MS system performance, e.g., mass shifts and slight variations in the laser focus size or fluence. Data pre-processing can involve isotope filtration, ion adduct grouping by morphological correlation, background signal subtraction, spectral smoothing, alignment, and mass recalibration. This is followed by peak picking and binning to create a unified data matrix. Various algorithms such as k-means, self-organizing maps, or hierarchical clustering can then decipher the complex information [13].

Next to commercial data analysis software, several open-source software solutions such as rMSI [20,21], Metaspace [22], Cardinal [23], LipidXplorer [24], or MZmine [25] are available. These can often be adapted for the sample system by advanced users. Challenges include the large data size generated by modern MS systems, particularly those with ion mobility separation (IMS) or ultra-high mass resolution features, and the integration of the reconstructed MSI with multimodal data such as high-resolution microscopy for accurate identification of regions of interest (ROI), which inherently steam from different machinery.

A major challenge at this stage is the accurate chemical identification of signals. Despite extensive preprocessing, annotations remain tentative when based solely on the accurate mass (MS1) supported by literature and databases such as METLIN, Human Metabolome Data Base (HMDB), LIPID MAPS, mzCloud, PubChem, and NIST. The task is to reach a higher level of confidence in the annotation, especially with lower mass accuracy [13,26]. In certain cases, tandem-MS (MS/MS) spectra can identify structural elements such as fatty chains and lipid headgroups to confirm the annotated lipid class.

3. MALDI-MSI in the study of atherosclerosis

Table 1 lists publications from the last decade that demonstrate the use of MALDI-MSI to analyze plaque histomolecular heterogeneity and metabolic profiles from arterial tissue affected by atherosclerosis. The researchers describe significant alterations in the abundances of identified biomarkers in distinct regions of the lesions.

Table 1
Approach and technical parameters of key publications using MALDI-MSI for the analysis of atherosclerosis in the past 10 years. Legend: ctrl: control (e.g., early-stage atheroma); repl: Technical replicates; HFD: Mice were fed with high fat diet to induce plaque growth; PBS: Phosphate buffered saline; PFA: submerged into paraformaldehyde for several minutes; DHB: 2,5-dihydroxybenzoic acid; CHCA: α-cyano-4-hydroxycinnamic acid; Nor: Norharmane, 9AA: 9-aminoacridine; DAN: 1,5-diaminonaphthalene; subl: Matrix applied by sublimation; HBSS: Home-built sublimation system; ImPrep: ImagePrep automatic matrix sprayer (BD); SunCol: SunCollect, SunChrom, Friedrichsdorf, Germany; SMPrep: SMALDIPrep, TransMIT GmbH, Gießen, Germany; HTX: TM Sprayer M3/M5, HTX, Chapel Hill, NC; HTXSbl: HTX Sublimator, HTX; SApp: Sublimation apparatus, Chemglass Life Science, Vineland, NJ; LMD: Tissue extracts isolated with laser capture microdissection; Sx: Sciex, Framingham, MA; BD: Bruker Daltonics, Bremen, Germany; OT: Orbitrap (Thermo Fisher Scientific, Bremen, Germany), BG: Background signal, e.g., from MALDI matrix clusters; GPrism: GraphPad Prism (GraphPad Software, La Jolla), NMF: non-negative matrix factorization for unsupervised clustering; HMDB: human metabolome data base; LM: LIPIDMAPS; IHC: Immunohistochemical staining.

	Model			Technical parameters					Identification			
	Sample system	N	Specimen and disease state	Sample preparation	Matrix	Instrumental parameters	Multi-modality	Targeted approach	Software	Databank	Staining and microscopy	Validation/ standards/level of confidence
42	human	9	stable and unstable atheromas with fibrous cap and necrotic core	fixed in form-aldehyde, embedded in paraffin, deparaff.	CHCA + TFA; DAN, spray, HTX M5	timsTOF fleX (BD) both ion modes pixel size 30 µm *m/z* 50-1000	RNA-seq	–	FlexImaging 5.1 (BD) SCiLS Lab Pro 2021b (BD) GPrism 9.0: Student *t*-test, Benjamini-Hochberg correction Stary Classification Scale scoring	Metabo-scape Metaspace HMDB	H&E, picrosirius red, Alizarin red, von Kossa	12 targeted MALDI-MS/MS on tissue section, standards
5	ApoE−/−mice	30	Aorta; advanced coronary disease Plaques with lipid-rich necrotic core	snap frozen in OTC	CHCA DHB subl. acoust. droplet	Synapt G2-S (Waters, MA) pos ion V-mode pixel size 50 µm *m/z* 50-950	LC-MS/MS from plasma extracts	Semi-targeted *d6*-Chol-esterol	BioMap 3.7.5.5 (Novartis, Basel)		H&E	*d6*-cholesterol orally administered
36	human	12	carotid artery endarterectomy plaques	snap frozen, embedded in gelatine desiccated	DHB subl., HBSS	Synapt G2-S (Waters, MA) resolution mode pixel-size 45 µm *m/z* 300–1200	Lipidyzer (Sx) MALDI-FTICR-MSI; solariX xR MS (BD)	–	MATLAB™ 2017a (Natick, MA) and mMass software: Isotope removal, nonnegative matrix factorization reduction. MeVisLab for corregistration multivariate analysis; OPLS-DA model SIMCA 15	Metaspace (FTICR) HMDB, LipidMaps, Swiss Lipids	Oil Red O, Miller's elastic Martius scarlet blue trichrome, and H&E	
29	human	30	coronary artery with intimal thickening (lipid pool), lipid core, or necrotic core	23 frozen and 21 paraffin-embedded specimens	DHB, spray, ImPrep	Autoflex III (BD) Linear TOF Pos. ion mode		CE18:2 CE18:1	FlexAnalysis & FlexImaging (BD) GPrism 6: Student *t*-test, 1-way ANOVA; Tukey multiple comparison Mann-Whitney *U* & Kruskal-Wallis with Dunn multiple comparison		Elastica van Gieson, Sudan IV, picrosirius red, IHC with several targets	
35	human	6	symptomatic and asymptomatic carotid plaques with lipid-necrotic core, calcification and hemorrhage	embedded in 2 % agarose	NOR DHB + 0.2 % TFA, spray, SunCol	Spectroglyph MALDI/ESI Injector on OT QExactive Plus Pos. ion mode *m/z* 150–2000		–	MATLAB: weak denoised, PCA and k-means clustering Partial least squares (PLS) Hierarchical clustering ORBIIMAGEmzXML2Tricks: peak picking and feature extraction	Metlin	Masson's Trichrome, H&E IHC against α-SMA & CD68	norharmane and DHB comparison
28	ApoE−/− mice at different ages, human	human 8 + 3ctrl mice 2–4	Human peripheral artery plaques, murine aorta or carotid artery	perfused with PBS embedded in gelatine	DHB, 0.1 % TFA, spray, SM-Prep	APSMALDI (TransMIT) on OT QExactive (HF) Pos ion mode pixel size: 5/15 µm *m/z* 300–1200		CE, CD, LPC, LPE	MSiReader V09-1 Mirion V3: mass errors, normalized to TIC, nonparametric Kruskal–Wallis intensities majorly simplified Perseus: for PCA	LipidMaps	H&E, Movat's pentachrome IHC against MAC387	
40	male New Zealand white rabbits, HFD	12	early atherosclerosis, ascending aortic sections	rinsed in PBS, snap frozen	DHB, 0.05 % TFA, 9AA	UltrafleXtreme (BD) pixel size 30 µm Pos. and neg. ion	Proteomics	–	FlexImaging 2.1 (BD) ClinProTools 3.0 (BD): smoothing, baseline subtraction, mass spectral alignment,	LipidMaps	H&E, red alizarin oil red O IHC against	distinct regions of interest (media, intima, plaque)

(*continued on next page*)

Table 1 (*continued*)

	Model			Technical parameters					Identification			
	Sample system	N	Specimen and disease state	Sample preparation	Matrix	Instrumental parameters	Multi-modality	Targeted approach	Software	Databank	Staining and microscopy	Validation/ standards/level of confidence
					spray, ImPrep	mode *m/z* 500–1200			normalization and recalibration GPrism: Mann–Whitney non-parametric test		α-actin & TMSB4X	exact mass on FT-ICR
33	C57BL/6J ApoE-/-, Ldlr-/- mice,	1	aortic root, plaques with necrotic core	snap-frozen	DHB + 1% TFA, HTXM3	RapifleX (BD)	several	–	re-calibrated SCiLS Lab 2016b (BD): linear discriminant analysis, PCA		H&E	
27	WHHL rabbit	1 with repl.	big and small lesion of thoracic aorta	snap frozen	DHB +1 % TFA, spray, airbrush	iMSCope; Shimadzu pos ion mode *m/z* 350–800	iMScope microscopy	synthetic standards	Imaging MS Solution 1.01.00 (Shimadzu): normalized to TIC ROIs by Welch's *t*-test		Oil Red O Mayer's hematoxylin solution	MALDI-MS/MS with chemical standards, Molecular species level indicated 12 *Ldlr*-/- mice, for LDL harvest
38	human	2/+ 1ctrl	advanced carotid endarterectomy plaques, cranial to the bifurcation	rinsed DPBS, snap frozen desiccated	DHB subl, HBSS	Synapt G2Si (Waters, MA) "resolution mode", pixel size 50 μm		–	HDimaging v1.4, MATLAB™ 2017a: TIC normalization, second-order Savitzky-Golay filter, re-calibration, mMass v5.5.0: baseline correction and peak picking, lipid fractional mass filter, Cross-Correlation-Based Peak Selection, ROI		H&E, Oil Red O, Resorcin-Fuchsin, IHC against CD31 and CD68	LC-MS/MS extracts Molecular species level indicated Odd-chain standards CE (17:0) and PC(17:0/17:0)
39	human	2/3repl	Severe aortic stenosis (AS) with calcified microdomains	immersion in ammonium formate	DHB subl, SApp	UltrafleXtreme (BD) Pos. ion mode *m/z* 300–1000 pixel size 30 μm	LC-MS/MS for proteomics	–	FlexImaging 4.0, BD TIC normalization ClinproTools: clustering analysis, Convex Hull baseline, Savitzky–Golay filter, recalibration	Lipid Blast	H&E	MALDI-MS/MS of four targeted lipids method set up with murine aorta
37	human	6	Carotid endarterectomy plaques with necrotic core	embedded into gelatin, 4 % PFA	DHB subl, HBSS	Synapt G2Si (Waters, MA) *m/z* 300-1200	Photo-acoustics, Lipidyzer platform	–	in-house pipeline: smoothing and recalibration, TIC normalization, BG removal	Metaspace	H&E Oil Red O	LC-MS/MS of homogenized CEA
31	Ldlr−/− mice, ApoE−/− mice	6/245 repl. (3D)	aortic roots lesions under specific diet	fresh-frozen in OCT 7 μm sections	NOR spray, HTX	RapifleX (BD) neg and pos ion mode	LMD on Spectroglyph Injector - OT	–	FlexControl 4.0, FlexImaging 5.0, FlexAnalysis v3.4 (BD) SCiLS Lab (BD): normalized to RMS, Pearson correlation mMass 5.5.013 for peak-picking, Deisotoping, BG removal		H&E	MS/MS of targeted lipids in LMD extracts
30	Ldlr−/− mice, with HFD, human	Mice 11/11 human 9	Aortic roots, early-stage & advanced carotid endarterectomy plaques	snap-frozen in OCT	9AA spray, SunCol NOR subl, HTXSbl	9.4TSolarix BD *m/z* 100-1000 timsTOF fleX *m/z* 340–1000 pixel size 10 μm neg ion mode	LC-MS/MS of human plasma	Semi-targeted LPA(18:1) LPC(18:0)	SCiLS Lab 2020a: Pearson correlation analysis mMass (v5.5.0): peak picking, smoothing, deisotoping ANOVA: mixed-effects models	HMDB, Metlin	H&E, oil red O, alizarin red S	on-tissue MALDI-MS/MS of targeted *m/z*
34	familial hypercholesterolemia swine, HFD	11/6	Mild, advanced, and control of coronary artery plaques	embedded in gelatine, snap frozen, dessicated	DHB, DAN; subl, HBSS	Synapt G2Si (Waters) 12T solariX (BD) Pixel size 45 μm *m/z* 300–1200		–	MassLynx v4.2 software, and HDI v1.4 (Waters) SCiLS Lab (BD) MATLAB™ 2017a and mMass: isotope filtering, NMF with k-means, SIMCA 17 (Umetrics): PCA and OPLS-DA; CV-ANOVA	LipidMaps	H&E, Oil Red O resorcin-fuchsin stain IHC against CD68	Exact mass with MALDI-FTICR-MSI

3.1. MSI analysis approaches

Most research groups did not perform targeted analyses, taking advantage of the untargeted nature of MSI, which allows for post-measurement signal identification. A few exceptions: Shen and co-authors focused on oxidized lipids in atherosclerotic lesions, supporting their detection with synthetic standards [27], whereas a few groups focused their semi-targeted analyses on cholesterol derivates, the glycerophospholipids (GPL) lysophosphatidylethanolamines and lysophosphatidylcholines [5,28,29] Cao et al. targeted one set of experiments on LPC(18:0) and LPA(18:1), identifying these lyso-GPLs as indicators of an altered phospholipid metabolism in atherosclerotic carotids [30].

3.2. Models for MSI experiments

Studies on atherosclerosis usually rely on animal models to gather insights into the initiation and progression of the plaque and identify biomarkers in distinct areas. These findings are then translated to human samples, illustrating the applicability of MSI in clinical scenarios. Common models for atherosclerosis are ApoE−/− (apolipoprotein-E deficient) mice [28,31], which have been shown to develop lesions similarly to humans with a plaque distribution mainly in the aorta, especially the aortic root, and the carotid artery [32]. Another common model are Ldlr−/− (low-density lipoprotein receptor-deficient) mice [31,33]. The mice are often given specific diets like high-fat diets (HFD) to induce the disease [5,28,31,33]. By treating wild-type C57BL/6-J mice with DHA liposomes, Chong et al. observed a similar development of plaques compared to ApoE−/− mice fed with regular chow [33]. Slijkhuis et al. highlighted the higher resemblance and thus better translation of familial hypercholesterolemia (FH) swine to humans. In their study, the FH swine on HFD developed complex plaques with varying sizes and compositions, similar to humans [34].

Human tissue from amputated limbs and corresponding controls steamed from carotid endarterectomy plaques or aortic lesions ranging from mild conditions such as pathologic intimal thickening to severe progression with necrotic core and calcified microdomains [29,35–39]. Khamehgir-Silz et al. compared lipid profiles of human atherosclerotic arteries with those of mice to determine universally applicable physiological biomarkers for the disease. They found several biomarkers unique to older ApoE−/−mice, whereas young ApoE−/− mice showed stronger similarities with wild-type mice [28]. Slijkhuis et al. discovered a strong resemblance in the lipid profiles of mildly diseased artery segments and control tissue, suggesting that this disease state was not lipid-driven but most atherosclerotic lesions might develop from intimal cell masses [34].

The sample size in the research presented varied from N = 1–2 with technical replicates [27,38,39] to the currently highest number of measured individuals within a line of research, which was N = 30 [5,29].

3.3. MALDI sample preparation and instrumentation

To date, there is no harmonized pipeline for analyzing atheroma with MALDI-MSI, largely due to ongoing fundamental developments of the technique. In some studies, specimens were perfused with phosphate buffer solution [28,38,40], snap-frozen, and, for accurate cryo-sectioning, in most cases, embedded in various media, including gelatine [28,36,37], agarose [35], paraffin [29], and OCT [5,31]. The use of OCT can be problematic for MALDI-MSI as it can cause severe ion suppression effects or overload the mass detector system with background ions of the polymers. Other researchers opted to not use embedding media [27,33,40]. Visscher et al. suggested an optimized protocol for tissue preparation and measurement, comprising desiccation under vacuum at room temperature after rinsing with buffer solution [38].

As a matrix, DHB or norharmane was used in most cases and applied through sublimation or spraying. In one comparative study, DHB produced more than three times the number of identified signals with also better morphological segmentation compared to norharmane [35]. Several studies added trifluoroacetic acid (TFA) to enhance ionization yields [27,28,33,35,40]. Visscher et al., however, recommended avoiding the addition of ionization agents as also any washing or re-crystallization [38].

Orthogonal time-of-flight analyzers (TOF) [19] from Bruker Daltonics, Shimadzu Cooperation, or Waters™ as well as orbitrap analyzers (Thermo Fisher™) are the MS systems of choice for most MALDI-MSI research, as also in the publications presented in this review. The typical mass range employed is m/z 300–1200, covering major lipid classes. Most research is limited to the (+)-ion mode only, presumably due to resource constraints. Cao and co-authors used both ion modes for a more comprehensive tissue characterization [31]. However, this study used a linear TOF, which, while offering superior analytical speed, sacrifices mass resolution and accuracy in signal annotation. On the contrary, MALDI-MSI performed on an Orbitrap mass analyzer was reported with a mass resolution of 240,000 @m/z200; using an AP-SMALDI5-AF ion source (TransMIT GmbH, Giessen), a few tissue sections could furthermore be analyzed with the smallest reported pixel size of down to 5 μm [28].

3.4. Data analysis

After data generation, the correct and comprehensive interpretation of the acquired data represents a major bottleneck of MALDI-MSI. Among the works presented, there is no common approach in the data analysis. Multivariate statistical analyses such as PCA or unsupervised classification are frequently employed to demonstrate compositional similarities within the sub-regions of atheromas [28,35,36]. These tools reveal coherences between, e.g., the inner VSMC region and the macrophage region, and furthermore differentiate symptomatic and asymptomatic cases, as illustrated in Fig. 4B [35].

While most studies rely on generic signal annotation of the measured m/z value as determined by vendor software using databases such as LIPIDMAPS, HMDB, or Metlin, some researchers used more comprehensive data analysis with METASPACE for data with high mass resolution [36,37]. Greco et al. generated project-specific data cubes that aligned filtered lists of all identified m/z values and registered common signals from all compared tissue sections to distinguish asymptomatic from symptomatic plaques [35]. Visscher et al. composed a pipeline to process both MSI and histological data to identify ROI and assessed the reproducibility of MSI measurements in the open.imzml format. Their data pipeline allowed for identifying both inter- and intra-section variations within a set of measured tissue sections [38]. Moerman et al. applied unsupervised nonnegative matrix factorization to reduce the dimensionality of the spectra and to extract major patterns with great coherence to the histological segmentation [36].

3.5. Level of confidence in lipid identification

Due to the challenging annotation of detected MSI signals, some researchers aimed for a higher level of identification confidence through tandem-MS or chemical standard substances. Castro et al. identified lipid contents using liquid chromatography (LC)-MS from lipid extracts [5,38] whereas Moerman et al. used the Lipidyzer platform (Sciex, Framingham, MA) [36] and Iskander-Rizk et al. utilized LC-MS/MS to analyze homogenized atherosclerotic tissue [37]. Guided laser-microdissection was used to precisely cut plaque areas to target lipids with MALDI-MS/MS in their extracts [31]. This offers the valuable trade-off of a less precise spatial analysis compared to MALDI-MS/MS but with improved MS/MS capabilities. Another approach is the measurement of small tissue sections with FT-ICR-MSI to determine the exact mass of previously measured compounds, increasing confidence in assigning detected signals to a lipid class [36,40].

Shen et al. uniquely confirmed several lipid identities directly with MALDI-MS/MS using lipid standards [27] whereas Lim et al. confirmed the identity of four target lipids by MALDI-MS/MS [39]. Considering stable isotope-labeled standards, the only reported work used cholesterol-d6 fed to mice to trace spatial and temporal lipid alteration in plaques. The approach not only achieved high level of confidence due to this chemical specificity but could also majorly aid the characterization of therapeutical treatments for plaque formation [5].

3.6. Multimodality in atherosclerosis MSI experiments

Most studies identified plaque symptomatology by combining MSI with classical histological stainings annotated by experienced pathologists to benefit from the higher spatial resolution [35,36]. Next to the ubiquitous hematoxylin-eosin staining, many studies employed more specific histological stains to enhance tissue annotation: Oil Red-O for overall lipid abundance [27,36–38,40], Masson's Trichrome for identifying vessels [35,41], and other specialized staining techniques. To highlight VSMCs and macrophages, several groups furthermore employed immunohistochemistry [29,35,38,40]. Greco et al. also demonstrated the value of combining MSI with fluorescence microscopy. This comprehensive approach defined seven functionally important regions of plaques: lipid-necrotic core, calcification, collagen-rich area, hemorrhage, macrophage-rich area, and inner and outer VSMCs. Integrating microscopic data with MSI data sets facilitated the identification of compositional similarity in lipid profiles across distinct regions but also specific lipid clusters associated with symptomatic and asymptomatic plaques. Notably, this approach highlighted macrophages as essential contributors to plaque inflammation, particularly as foam cells [35].

Iskander-Rizk et al. showcased a new micro-spectroscopic photoacoustic imaging set-up to explore spatial lipid signatures within plaques at a microscopic level, validated by MALDI-MSI [37]. Another notable study by Seeley et *al.* combined RNA-sequencing with MSI to compare stable and unstable human atherosclerosis. By integrating publicly available RNAseq data, they annotated 170 spatially resolved metabolites, many of which had not been associated with atherosclerosis before. They proposed several metabolite classes that might contribute to plaque instability, in contrast to a maintained metabolic activity related to lipids and long-chain fatty acids in stable plaque [42]. Further multimodal research was presented by combining lipidomic and proteomic approaches to gain insights into lesion progression, such as the transition from non-calcified to calcific disease in severe atherosclerosis [39,40].

3.7. 3D reconstruction of atherosclerotic lesions with MALDI-MSI

Three-dimensional chemical reconstruction of affected vessels represents an advanced approach in MSI-based investigations. Since plaques grow asymmetrically, a 2D section alone cannot fully capture the disease state, and the volumetric variability of up/down regulated biomarkers might be missed or described incorrectly. These alterations in lipid distribution along the plaque can be captured by performing MALDI-MSI of numerous consecutive sections (Fig. 3). Measuring over 100 consecutive sections, this technique requires sophisticated data reconstruction and analysis. The approach provided valuable insights into the stenosis growth within the aorta of two mice, or human carotid artery, respectively [31,43]. However, Visscher et al. did not observe significant longitudinal variations in a coarser series of sections within 1 mm segments [38]. Given that the disease is often prone to regions of turbulent blood flow such as bifurcations [1], 3D-imaging could be an important contributor to elucidate these phenomena.

4. Lipids and their spatial distribution in the progression of atherosclerosis

Atherosclerosis is majorly considered a lipid-mediated pathology [7]. Multiple specific lipids have a prominent role in the progression of atherosclerosis [44,45]. The spatial information and parallel detection features of MALDI-MSI add a new dimension to this atlas of knowledge: Recent MALDI-MSI research highlighted the correlation of inflammation with the formation of vulnerable plaques, rupture of fibrous caps, and the resulting symptomatic manifestation of atherosclerosis. These studies uncovered distinct lipid signatures as potential drivers of plaque destabilization and disease progression.

Table 2 lists lipid species that were reported to be significant for atherosclerosis analyzed with MALDI-MSI in the corresponding affected specimen, with the main groups reported being GPLs, lyso-GPLs, cholesterols, derivates and CEs, sphingolipids, and glycerolipids. The untargeted approach of MALDI-MSI can lead to the detection of many features of this highly diverse analytical class: Moerman et al. reported the spatial distribution of as many as ~200 signals for lipids from 106 tissue sections that they could assign to 93 unique lipid species [36]. Iskander-Rizk et al. showed the distribution of ~70 lipids in human CEA plaques [37], and Seeley et al. identified 170 lipids and further metabolites of which more than 60 showed distinct differences between stable and unstable atheromas [42]. A noteworthy finding involved stable isotope labeled cholesterol, which, unlike free cholesterol, was not evenly distributed within atheromas following oral uptake [5]. Another is the identified dysregulation of lipid biomarkers not only in the atherosclerotic plaque but coherently also in adjacent tissue such as the heart tissue or aortic valve cusps [30,43].

4.1. Cholesterol and cholesterol derivates

The major constituents of atherosclerotic plaques are cholesterol and its derivates, including cholesterol esters such as CE(16:1), CE(18:1), CE (18:2), and CE(20:4) [5]. These sterols exhibit moderate spatial correlation and a clear distinction within different histological regions [36]. CE(18:1) has been associated with early-stage plaques, whereas CE (18:2) on the contrary was significantly more abundant in advanced plaques [38]. Slijkhuis et al., on the contrary, observed that both CE (18:1) and CE(18:2) co-localized with inflammatory tissue regions (identified through CD68-IHC staining) in advanced atherosclerotic tissue from FH swine [34]. Acetylated cholesterylsteryl glucosides were proposed as a new class of biomarkers for atherosclerotic peripheral arteries in humans [28]. Additionally, intimal VSMC in symptomatic plaques were found enriched in cholesterol and CEs, indicating an induced lipid uptake [35], while calcified microdomains in aortic stenosis showed a decreased cholesterol content [39]. Furthermore, toxic oxysterols such as 27-hydroxycholesterol and 7-ketocholesterol were described as major contributors to atherosclerotic progression [27,34].

4.2. Glycerophospholipids

Several species of lyso-GPL, especially lyso-PC, could be associated with significant roles in the advance of the disease, particularly linked to inflammation or oxidative stress: LPC(16:0), LPC(18:0), and LPC(18:1) were majorly upregulated in the lesion regions [27,43], indicating an inflammatory response [5,34,39], calcified microdomains [39], and vascular destabilization [5]. They were furthermore upregulated in the macrophage regions of symptomatic plaques [35], and were proposed as markers for human atherosclerotic lesions, potentially translatable to mouse models [28]. LPA(18:1), LPA(20:1), LPE(O-18:1), LPE(18:0), LPC (18:2), and LPI(18:0) were identified as plaque-specific across all three dimensions of the plaque [31], suggesting an altered phospholipid metabolism in the atherosclerotic tissue [30].

In addition, LPC(18:0) and LPA(18:1), in particular, colocalized within the necrotic regions and foam cells and were validated for their

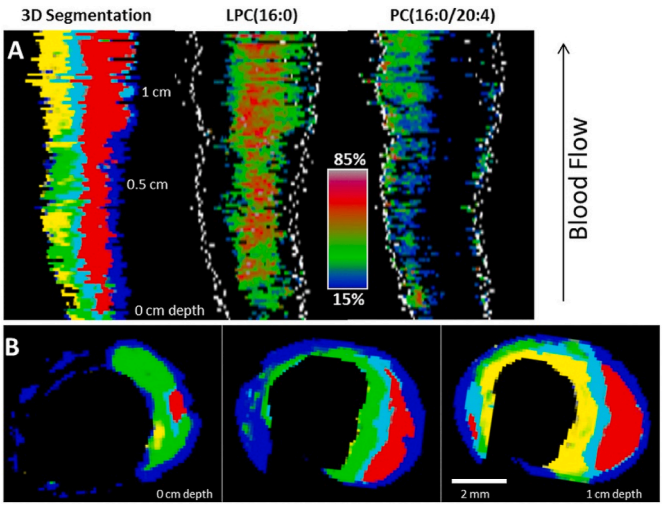

Fig. 3. Longitudinal MALDI-MSI 3D visualization of lipid distribution in human carotid atherosclerotic plaque showing the evolution of the molecular histology for a total length of 1.18 cm with increasing stenosis. (A). 3D longitudinal view along an affected vessel showing the segementation of MS data in different plaque regions as also the distribution of LPC(16:0) and of PC(36:4) the same depth plane distinguishing the yellow and red segments. (B) Axial sections from increasing depth showing the segment images in the plaque [43]. ©Wiley. (For interpretation of the references to colour in this figure legend, the reader is referred to the Web version of this article.)

translational potential in human blood plasma [30]. LPA species were moreover suggested as precursors to PA localized in calcified areas [40].

The higher molecular PC species were often highly correlated and showed only a weak correlation with LPCs. PCs were primarily located around the lumen and occasionally found migrating into thrombotic or inflamed regions [36,43]. In the lipid-necrotic core, PC abundance was notably decreased [35], whereas PE-Os, in contrast, were reported with high abundance [34]. Also, PA-O and PI-O were shown to be upregulated in the lipid-necrotic core [34], but we stress that rare ether lipid species as such require further identity confirmation to reach a sufficient level of confidence [13] and provide evidence of their roles as specific biomarkers (see chapter below).

4.3. Sphingolipids

The regions with the most significant changes in lipid composition associated with plaque outcome are inner VSMC, macrophage-rich regions, and the lipid-necrotic core [34,35]. An important class of lipids here is SM. SM(34:2) was found to be highly abundant in macrophage-rich regions of symptomatic lesions and associated with lipid raft formation, inflammation processes, and plaque instability. The high abundance of SM or PE-ceramides in the lipid-necrotic core is attributed to the macrophages' conversion into apoptotic foam cells [35]. Additionally, Cao et al. defined SM(d34:0; 2) as plaque-specific in all three plaque dimensions [31]. PE-ceramides and ceramide-1-phosphates (CerP) were reported to co-localize with LPC species in human plaque [43], and specifically PE-Cer(38:1), CerP (d34:1) and CerP(d36:1) were suggested as atherosclerotic biomarkers [30,34].

4.4. Glycerolipids

DG and TG species exhibited a different spatial distribution compared to most lipid classes, except for certain CE species [36]. DG were higher concentrated in thrombotic areas than in other plaque regions [38]. Given that the heart primarily uses fatty acids (FA) as an energy source, these lipids could serve as potential biomarkers, making them a valuable analytical target [7].

4.5. Polyunsaturated fatty acids

Polyunsaturated fatty acids (PUFAs) or PUFA-containing lipids are potential precursors to pro- and anti-inflammatory oxylipins and thus could be important components in the plaque formation [46–48].

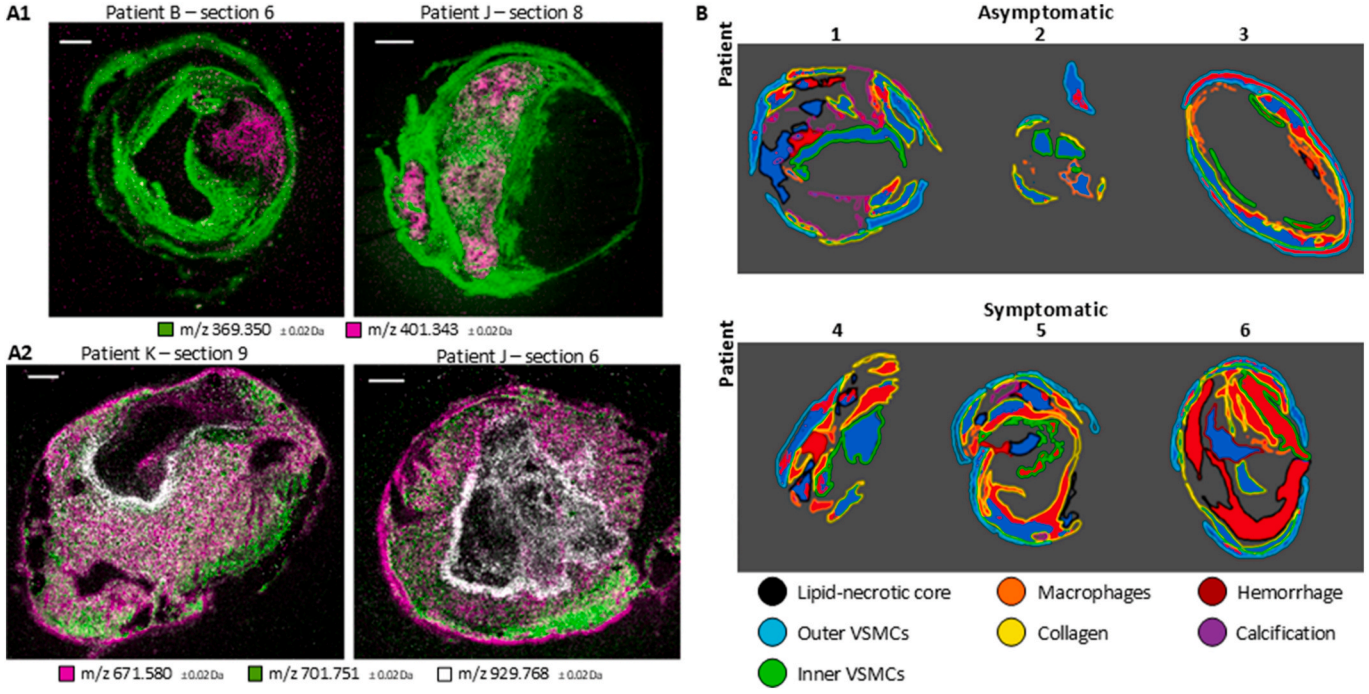

Fig. 4. MALDI-MSI from atherosclerotic vessels (adapted). (A): Spatial distribution of (a1) 7-ketocholesterol (purple) and cholesterol (green), (a2) a CE (purple), a SM (green), and a TG in white [36]. (B): k-means cluster analysis discriminating distinct regions for asymptomatic and symptomatic plaque [35]. ©Elsevier; MDPI. (For interpretation of the references to colour in this figure legend, the reader is referred to the Web version of this article.)

Table 2
Lipid species that have been reported to be specific for atherosclerotic plaques by several work groups (indicated reference). * = confirmed with MS/MS from tissue extracts, # = confirmed with on-tissue MALDI-MS/MS.

		Human atherosclerotic plaques					Animal atherosclerotic plaques			
Lipid species		carotid	aortic	carotid trombus	limb arterie	LC-MS/MS homogenate	ApoE−/− mice	Ldlr−/− mice	WHHL rabbit	FH swine
Glycerophospholipis	LPC 16:0	36*, 37					5, 31*	31*	27#	34
	LPC 18:0	*30**, 36*, 37					5, 31*	30#*, 31*	27#	
	LPC 18:1	36*, 37					5, 31*	31*	27#	34
	LPC 18:2	35, 36*, 37			28		28, 31*	31*	27#	34
	LPC 18:3	36*, 37					28			34
	LPC 20:3	36*			28		28			34
	LPC 20:4	35, 36*, 37								
	LPC 20:5	36*, 37								
	LPE 18:0				28		28, 31*	31*		
	LPI 18:0						31*	30, 31*		34
	PA 34:1	35	14					30		34
	PC 32:0	35, 36*, 37*, 38*				38*			27#	34
	PC 34:1	35, 36*, 37*, 38*								34
	PC 34:2	35, 36*, 37*, 38*				38*			27#	34
	PC 36:1	37, 38*				38*				34
	PC 36:2	37*,38*				38*			27#	34
	PC 36:3	35, 36*, 37*, 38*				38*				34
	PC 36:4	27, 35–38*				38*				
	PC 38:4	35, 37, 38*				38*				34
	PC O-36:4	37, 36*								34
	PC O-36:5	37, 36*								34
	PI 34:2							30		34
Sterols	cholesterol	35, 36*, 37, 38*				38	5	30	27#	34
	7-ketochol.	36*, 37								34
	CE 16:0	37*			28	38*	28			
	CE 16:1	37*			28	38*	5, 28			
	CE 18:1	29, 37*				38*	5	30		34
	CE 18:2	29, 35, 37*, 38*			28	38*	5, 28	30	27#	34
	CE 20:1				28	38*	28			
	CE 20:3	37			28		28			
	CE 20:4	36, 37*			28		5, 28			
	CE 20:5	35, 37*			28		28			
	CE 22:5	36, 37*				38*				
	CE 22:6	36, 37*			28		28			
	HODE-CE	37*					28		27#	
Sphingolipids	PE-Cer d36:1	35	14							34
	CerP d34:1							30		34
	SM d34:0	36*					31*	30, 31*		34
	SM d34:1	35, 36*, 37*, 38*				38		30	27#	34
	SM d34:2	35, 36*						30		
	SM d36:1	36*, 37*, 36				38				
	SM d40:2	35, 37*								
	SM d42:2	35, 37*, 38*				38*				34
Glycerolipids	DG 32:0	36		38						
	DG 32:1	36, 37		38						
	DG 34:0	36		38						
	DG 34:1	36, 37*		38						
	DG 34:2	36, 37*		38						
	DG 36:2	36, 37*, 38		38						
	DG 36:3	36, 37*		38						
	DG 36:4	36, 37*		38						
	DG 38:4	36		38						34
	TG 52:2	36, 37*, 38								34

Tanaka et al. investigated on the arachidonyl-PC metabolism in human and mouse atherosclerotic tissue with MALDI-MSI. Monitoring LPC and arachidonyl-PC, they showed an anti-correlation of the PUFA-containing lipid, and a dysregulation of LPC-acyltransferase-3 with disease progression. MSI moreover helped to localize an accumulation of arachidonyl-PC to VSMCs [49]. The saturated stearic acid and palmitic acid, in contrast, may increase VSMC modulation, enhancing proinflammatory responses in macrophages [42]. Chong et al. demonstrated the use of DHA liposomes to inhibit inflammation and induce macrophage foam cell formation in vitro, suggesting a potential therapeutic application for liposomal DHA [33].

Oxylipins that can be detected with MALDI-MS were recently published in a dedicated library [50]. As these lipid species and their generation from PUFA expose a crucial but ambivalent influence on the

atherogenesis [48], unraveling their spatial distribution can majorly assist atherosclerosis research: Nakagawa et al. reported polyunsaturated PC(36:4) with low intensity in the deeper layer of advanced lesions, whereas the oxidized species PC(16:0/9:0(CHO)) and PC (16:0/9:0(COOH)) were found to be evenly distributed. In combination with immunohistochemistry, they could relate the accumulation of oxylipins to the development of Mox macrophages [29]. As recently shown with desorption electrospray ionization (DESI)-MSI, FFAs were localized predominantly in the shoulder regions of plaques, which are rich in macrophages. This suggests that a balance between pro-inflammatory saturated FFAs and polyunsaturated fatty acids (PUFAs) may play a role in stabilizing atherosclerotic plaques [51].

5. Challenges in the analysis of atherosclerosis

Several challenges limit the analytical depth of tissue characterization with MALDI-MSI, and the extent of technical and biological variance has yet to be evaluated. The complex measurement procedures in MALDI-MSI experiments often require a careful allocation of research effort, and researchers must evaluate trade-offs to reach robust hypotheses.

5.1. Tissue sampling

The heterogeneity of atherosclerotic lesions presents a significant challenge, as any 2-dimensional section might miss important contributors to plaque rupture. 3-dimensional analyses address this limitation [31] but require substantial technical effort. Accordingly, the small morphological features of lesions limit the comparability of consecutive cuts for multimodal approaches. Sampling furthermore requires greatest care to accurately reflect the in vivo state, for which no ultimate protocol could yet be defined.

In postmortem specimen, small changes in the metabolite profiles can be detected [42], but these cannot be directly extrapolated to the living state. Seeley et al. suggested collecting samples from living human donors. Sample fixation with FFPE plus downstream deparaffinizing can preserve the morphology, but significantly alters the biochemical composition, including the removal of crucial features like cholesterol and its derivates [42]. Furthermore, metabolic profiles can differ significantly between species such as mice and humans, as well as among individuals of different ages [28].

5.2. Data production and identification

A major challenge of MALDI-MSI is the concerted ionization/ablation process, in which all ionic species are generated and detected simultaneously. For this, important disease-related contributors might not be detected but might be excluded from the analysis due to high-abundant ion species or suffer from ion suppression effects in the complex chemical environment [52].

Moreover, detected signals cannot always be unequivocally identified, as near-isobaric or isomeric ion species cannot be distinguished [28]. For example, an ion m/z 782.568 could correspond to either $[PC(34:1) + Na]^+$ or $[PC(36:4) + H]^+$ – the difference between the sodiated and the longer-chain protonated ion is only 2.4 mDa, and both are likely to be produced within the (+)-MALDI process. Tandem-MS measurements can provide a higher confidence of annotation but are time-consuming due to the multeity of detected compounds [28]. Moreover, in-source fragmentation in MALDI-MSI cannot be excluded, and, e.g., the signals for PA, DAG or lyso-GPL could partially originate from dissociated PC or PE species. Accordingly, the characteristic in-source fragmentation product for cholesterol - m/z 369.35 (corresponding to the $[M\text{-}H_2O + H]^+$ ion) - could likewise originate from cholesterol derivates [35]. Visscher et al. leveraged this limitation with precursor ion scans determining the content of CE, PC, and SM, albeit from lipid extracts [38]. Few researchers combined measurements in both ion modes, which can identify a broader range of biochemical features that cannot be detected in the predominant (+)-ion mode alone [31,40].

LC-MS/MS of homogenized tissue extracts allows for confident lipid identification [37,38], but sacrifices spatial information. Ideally, direct MALDI-MS/MS from tissue sections, supported by authentic lipid standards, validates the suggested spatial identification of biomarkers while preserving the native ionization properties of compounds in tissue [27,39]. Low abundant signals, however, remain undetected due to low ionization yields or insufficient MS sensitivity [36], especially at higher spatial resolutions, where the ablated volumes per pixel are significantly reduced.

Chemical standards are invaluable for accurately identifying targeted compounds in any MS measurement [5,27,38,42]. However, the use of standards for quantitative analysis in MALDI-MSI remains an ongoing challenge. The extraction of analytes into the matrix and their subsequent ablation/ionization is highly dependent on the biochemical microenvironment of the analyte, which aggravates the quantification approach [53].

Recent technical advancements can majorly augment the analytical depth: Laser micro-dissection [31] and other multimodalities have already demonstrated promising enhancements of tissue characterization (see section 4). Yet, the integration of further orthogonal techniques such as in-vivo NMR from biological fluids is still pending. In other fields of MALDI-MSI, ion mobility and postionization techniques have significantly increased the number of detectable compounds [10]. Since the introduction of commercial MALDI-2-MSI instruments offering routine analyses with IMS and a spatial resolution down to 5 μm [54], the application of postionization for atherosclerosis research is highly anticipated, e.g., to elucidate the ambivalent role of ceramides [55] or oxylipins [8,50] with MALDI-PI-MSI [56].

Lastly, a large number of detected compounds remain unidentified due to the absence of the analyte in existing databases, or since the detected ion adduct cannot be deconvoluted [28,42]. The limitations of current reference platforms and databases underscore the need for continued research and development in this area.

5.3. MALDI-MSI in clinical application

MALDI-MSI for the analysis of atherosclerosis remains primarily in the realm of fundamental research and pilot studies, with its integration into clinical routine analysis still forthcoming. One major pending challenge is the lack of harmonized analytical protocols, including sample preparation, matrix and additive selection, instrumental parameters, and data analysis. The variability in research design across studies limits comparability. This extends to the integration of multimodal approaches, such as simple staining techniques, or more sophisticated approaches like RNAseq [42], for which unified approaches are pending.

For a broader clinical adoption of MALDI-MSI, methodological challenges related to cost, scalability, and automation of data processing must also be addressed. This is particularly true for the simultaneous integration of MALDI-MSI with spatial transcriptomics and proteomics. Additionally, human factors such as genetic background, lifestyle, diet, and comorbidities necessitate a significantly larger number of coherently measured atherosclerosis samples to reach sufficient validation and ultimately pave the way for the clinical implementation of MALDI-MSI.

6. Conclusion – the opportunities and expectations of MALDI-MSI

MALDI-MSI has been demonstrated to be a powerful tool for unraveling the complex morphology of heterogeneous atherosclerotic plaques in recent years. Co-localizing target analyte classes and distinct biomarkers within specific plaque regions has provided an

unprecedented understanding of different stages of the disease and the underlying metabolic processes and pathophysiology – insights that were unattainable before the advent of MSI – such as that the formation of lipo-necrotic tissue is majorly influenced by macrophages as well as a result of the focal structural collapse of the lipid core an atheroma.

Current research has led to a continuous workflow optimization, enhancing analytical throughput, comparability, and technical advancements: Khamehgir-Silz et *al.* demonstrated the morphological complexity of plaques with high spatial resolution down to 5 μm [28], setting the stage for transmission-mode MALDI-MSI to elucidate molecular structures down to single cell level [57]; the third dimension demonstrated the heterogeneous development of plaques. [43],31 These innovative approaches require significant effort but have already unraveled concealed atheroma features. Moving forward, the integration of modern techniques such as IMS [54] to enhance signal annotation accuracy, nanostructured LDI matrices [17,43,58], and postionization techniques [56,59,60] will majorly expand the range of detectable lipid classes.

The combination with multimodal approaches allows for a more comprehensive understanding of the progression of atherosclerosis and facilitates the application to further fields: For instance, Chong et al. utilized MSI to identify tissue regions based on the liposome fingerprint [33]. Doppler et al. investigated degenerative thoracic aortic aneurysms, revealing lipid-mediated and noncanonical atherosclerotic alterations as the driving force in the disease progression [61], whereas McDonald et al. investigated the spatial biochemistry of blood clots and murine thrombi ex vivo [62], further expanding the scope of MALDI-MSI in biomedical research.

For future studies, it will be crucial to maintain rigorous control over every step of the measurement pipeline, to avoid tissue degradation and enhance technical robustness. Implementing quality controls and harmonizing both technical and computational protocols will validate the gain of information and inter-laboratory transfer, and uncover critical parameters, such as the age of individuals and the level of interspecies comparability with humans [28].

Exact quantification and annotation remain a pending question for MALDI-MSI. For this, we believe that the available standardization and tandem-MS capabilities should be further explored to support tentative annotations of biomarkers and describe their accurate biological function within the complex disease environment. Key features identified through research should furthermore be compiled into databases or integrated into a comprehensive atlas of metabolic pathways, as recently suggested [42].

Altogether, we anticipate that presented research advancements with key factors, including validated protocols, simplification, and the ongoing commercialization of technical components will pave the way for the expansion of MALDI-MSI in clinical settings in the near future. As seen in other clinical areas, f.e., in non-invasive imaging studies, AI will be an increasingly vital component in clinical MSI [63].

The augmented depth of analytical information provided by MALDI-MSI will furthermore translate to related diseases, such as diabetes, obesity or non-alcoholic fatty liver disease, significantly enriching our understanding of the physiological processes involved [15]. Ultimately, hold the potential to reduce invasive surgery, highlight key factors in lifestyle and diet to prevent plaques formation, and substantially improve the clinical treatment of patients affected by this debilitating disease.

Author contributions

C.H.M.B.: Conceptualization, writing – original draft, review & editing, investigation; F.X.C.B.: Conceptualization, writing – original draft; L.M.: writing – review; P.M.: writing – review; O.Y.T.: writing – review; M.V.C.: Conceptualization, writing – original draft, review & editing.

Financial Support

The work by C.B has been supported by the European Union (MASS2 101067953 - HORIZON-MSCA-2021-PF-01). M.V is supported in part by Ministerio de Ciencia e Innovación (PID2022-136226OB-I00, CPP2022-010039) and the European Union (CardioSCOPE 10108639 - HORIZON-MSCA-2021-SE-01-01 MSCA Staff Exchanges 2021). The work of P.M. is supported in part by the European Union (CardioSCOPE 10108639 - HORIZON-MSCA-2021-SE-01-01 MSCA Staff Exchanges 2021, AtheroNET COST Action CA21153), the Italian Space Agency (ASI; N. 2023-7-HH.0 CUP F13C23000050005 MicroFunExpo) and the Italian Ministry of Health (project PNRR-MCNT2-2023-12377808, PNRR: M6/C2_CALL 2023), AtheroNET COST Action CA21153). Co-funded by the European Union. Views and opinions expressed are however those of the author(s) only and do not necessarily reflect those of the European Union. Neither the European Union nor the granting authority can be held responsible for them.

Declaration of interests

The authors declare that they have no known competing financial interests or personal relationships that could have appeared to influence the work reported in this paper.

Acknowledgements

We thank Maria Garcia-Altares Pérez for the provision of the MSI figures of the graphical abstract.

References

[1] J.L.M. Björkegren, A.J. Lusis, Atherosclerosis: recent developments, Cell 185 (10) (2022) 1630–1645, https://doi.org/10.1016/j.cell.2022.04.004.
[2] B.A. Ference, H.N. Ginsberg, I. Graham, et al., Low-density lipoproteins cause atherosclerotic cardiovascular disease. 1. Evidence from genetic, epidemiologic, and clinical studies. A consensus statement fromthe European Atherosclerosis Society Consensus Panel, Eur. Heart J. 38 (32) (2017) 2459–2472, https://doi.org/10.1093/eurheartj/ehx144.
[3] J. Borén, M. John Chapman, R.M. Krauss, et al., Low-density lipoproteins cause atherosclerotic cardiovascular disease: pathophysiological, genetic, and therapeutic insights: a consensus statement from the European Atherosclerosis Society Consensus Panel, Eur. Heart J. 41 (24) (2020) 2313–2330, https://doi.org/10.1093/eurheartj/ehz962.
[4] Y. Wang, J.A. Dubland, S. Allahverdian, et al., Smooth muscle cells contribute the majority of foam cells in ApoE (apolipoprotein E)-Deficient mouse atherosclerosis, Arterioscler. Thromb. Vasc. Biol. 39 (5) (2019) 876–887, https://doi.org/10.1161/ATVBAHA.119.312434.
[5] J. Castro-Perez, N. Hatcher, N. Kofi Karikari, et al., In vivo isotopically labeled atherosclerotic aorta plaques in ApoE KO mice and molecular profiling by matrix-assisted laser desorption/ionization mass spectrometric imaging, Rapid Commun. Mass Spectrom. 28 (22) (2014) 2471–2479, https://doi.org/10.1002/rcm.7039.
[6] A. Anderson, A. Campo, E. Fulton, A. Corwin, W.G. Jerome, M.S. O'Connor, 7-Ketocholesterol in disease and aging, Redox Biol. 29 (2020), https://doi.org/10.1016/j.redox.2019.101380.
[7] S.T.P. Mezger, A.M.A. Mingels, O. Bekers, B. Cillero-Pastor, R.M.A. Heeren, Trends in mass spectrometry imaging for cardiovascular diseases, Anal. Bioanal. Chem. 411 (17) (2019) 3709–3720, https://doi.org/10.1007/s00216-019-01780-8.
[8] A.C.A. dos Santos, D. Vuckovic, Current status and advances in untargeted LC-MS tissue lipidomics studies in cardiovascular health, TrAC, Trends Anal. Chem. 170 (2024) 117419, https://doi.org/10.1016/j.trac.2023.117419.
[9] A.R. Buchberger, K. DeLaney, J. Johnson, L. Li, Mass spectrometry imaging: a review of emerging advancements and future insights, Anal. Chem. 90 (1) (2018) 240–265, https://doi.org/10.1021/acs.analchem.7b04733.
[10] K.K. Krestensen, R.M.A. Heeren, B. Balluff, State-of-the-art mass spectrometry imaging applications in biomedical research, Analyst (2023), https://doi.org/10.1039/d3an01495a. Published online.
[11] S. Mas, D. Touboul, A. Brunelle, et al., Lipid cartography of atherosclerotic plaque by cluster-TOF-SIMS imaging, Analyst 132 (1) (2007) 24–26, https://doi.org/10.1039/B614619H.
[12] A.P. Bowman, R.M.A. Heeren, S.R. Ellis, Advances in mass spectrometry imaging enabling observation of localised lipid biochemistry within tissues, TrAC, Trends Anal. Chem. 120 (2019) 115197, https://doi.org/10.1016/j.trac.2018.07.012.
[13] G. Baquer, L. Sementé, T. Mahamdi, X. Correig, P. Ràfols, M. García-Altares, What are we imaging? Software tools and experimental strategies for annotation and identification of small molecules in mass spectrometry imaging, Mass Spectrom. Rev. 42 (5) (2023) 1927–1964, https://doi.org/10.1002/mas.21794.

[14] M. Martin-Lorenzo, G. Alvarez-Llamas, L.A. McDonnell, F. Vivanco, Molecular histology of arteries: mass spectrometry imaging as a novel ex vivo tool to investigate Atherosclerosis, Expert Rev. Proteomics 13 (1) (2016) 69–81, https://doi.org/10.1586/14789450.2016.1116944.
[15] A. Worthmann, A. Bartelt, MALDI MSI for a fresh view on atherosclerotic plaque lipids, Pflugers Arch 474 (2) (2022) 185–186, https://doi.org/10.1007/s00424-021-02654-8.
[16] J. Leopold, P. Prabutzki, K.M. Engel, J. Schiller, A five-year update on matrix compounds for MALDI-MS analysis of lipids, Biomolecules 13 (3) (2023) 546, https://doi.org/10.3390/biom13030546.
[17] P. Ràfols, D. Vilalta, S. Torres, et al., Assessing the potential of sputtered gold nanolayers in mass spectrometry imaging for metabolomics applications, PLoS One 13 (12) (2018), https://doi.org/10.1371/journal.pone.0208908.
[18] S.R. Ellis, S.H. Brown, M. in het Panhuis, S.J. Blanksby, T.W. Mitchell, Surface analysis of lipids by mass spectrometry: more than just imaging, Prog. Lipid Res. 52 (4) (2013) 329–353, https://doi.org/10.1016/j.plipres.2013.04.005.
[19] K.M. Engel, P. Prabutzki, J. Leopold, et al., A new update of MALDI-TOF mass spectrometry in lipid research, Prog. Lipid Res. 86 (2022) 101145, https://doi.org/10.1016/j.plipres.2021.101145.
[20] P. Ràfols, S. Torres, N. Ramírez, et al., RMSI: an R package for MS imaging data handling and visualization, Bioinformatics 33 (15) (2017) 2427–2428, https://doi.org/10.1093/bioinformatics/btx182.
[21] P. Ràfols, B. Heijs, E. Del Castillo, et al., RMSIproc: an R package for mass spectrometry imaging data processing, Bioinformatics 36 (11) (2020) 3618–3619, https://doi.org/10.1093/bioinformatics/btaa142.
[22] A. Palmer, P. Phapale, I. Chernyavsky, et al., FDR-controlled metabolite annotation for high-resolution imaging mass spectrometry, Nat. Methods 14 (1) (2017) 57–60, https://doi.org/10.1038/nmeth.4072.
[23] K.A. Bemis, M.C. Föll, D. Guo, S.S. Lakkimsetty, O. Vitek, Cardinal v.3: a versatile open-source software for mass spectrometry imaging analysis, Nat. Methods 20 (12) (2023) 1883–1886, https://doi.org/10.1038/s41592-023-02070-z.
[24] R. Herzog, K. Schuhmann, D. Schwudke, et al., LipidXplorer: a software for consensual cross-platform lipidomics, PLoS One 7 (1) (2012) e29851, https://doi.org/10.1371/journal.pone.0029851.
[25] R. Schmid, S. Heuckeroth, A. Korf, et al., Integrative analysis of multimodal mass spectrometry data in MZmine 3, Nat. Biotechnol. 41 (4) (2023) 447–449, https://doi.org/10.1038/s41587-023-01690-2.
[26] G. Baquer, L. Sementé, P. Ràfols, et al., rMSIfragment: improving MALDI-MSI lipidomics through automated in-source fragment annotation, J Cheminform 15 (1) (2023) 80, https://doi.org/10.1186/s13321-023-00756-2.
[27] L. Shen, T. Yamamoto, X.W. Tan, et al., Identification and visualization of oxidized lipids in atherosclerotic plaques by microscopic imaging mass spectrometry-based metabolomics, Atherosclerosis 311 (2020) 1–12, https://doi.org/10.1016/j.atherosclerosis.2020.08.001.
[28] P. Khamehgir-Silz, S. Gerbig, N. Volk, et al., Comparative lipid profiling of murine and human atherosclerotic plaques using high-resolution MALDI MSI, Pflugers Arch 474 (2) (2022) 231–242, https://doi.org/10.1007/s00424-021-02643-x.
[29] K. Nakagawa, M. Tanaka, T.H. Hahm, et al., Accumulation of plasma-derived lipids in the lipid core and necrotic core of human atheroma: imaging mass spectrometry and histopathological analyses, Arterioscler. Thromb. Vasc. Biol. 41 (11) (2021) E498–E511, https://doi.org/10.1161/ATVBAHA.121.316154.
[30] J. Cao, M. Martin-Lorenzo, K. van Kuijk, et al., Spatial metabolomics identifies LPC (18:0) and LPA(18:1) in advanced atheroma with translation to plasma for cardiovascular risk estimation, Arterioscler. Thromb. Vasc. Biol. 44 (3) (2024) 741–754, https://doi.org/10.1161/ATVBAHA.123.320278.
[31] J. Cao, P. Goossens, M. Martin-Lorenzo, et al., Atheroma-specific lipids in ldlr-/- and apoe-/-mice using 2D and 3D matrix-assisted laser desorption/ionization mass spectrometry imaging, J. Am. Soc. Mass Spectrom. 31 (9) (2020) 1825–1832, https://doi.org/10.1021/jasms.0c00070.
[32] S. Oppi, T.F. Lüscher, S. Stein, Mouse models for atherosclerosis research—which is my line? Front. Cardiovasc. Med. 6 (2019) https://doi.org/10.3389/fcvm.2019.00046.
[33] S.Y. Chong, X. Wang, L. van Bloois, et al., Injectable liposomal docosahexaenoic acid alleviates atherosclerosis progression and enhances plaque stability, J. Contr. Release 360 (2023) 344–364, https://doi.org/10.1016/j.jconrel.2023.06.035.
[34] N. Slijkhuis, F. Razzi, S.A. Korteland, et al., Spatial lipidomics of coronary atherosclerotic plaque development in a familial hypercholesterolemia swine model, J. Lipid Res. 65 (2) (2024) 100504, https://doi.org/10.1016/j.jlr.2024.100504.
[35] F. Greco, L. Quercioli, A. Pucci, et al., Mass spectrometry imaging as a tool to investigate region specific lipid alterations in symptomatic human carotid atherosclerotic plaques, Metabolites 11 (4) (2021), https://doi.org/10.3390/metabo11040250.
[36] A.M. Moerman, M. Visscher, N. Slijkhuis, et al., Lipid signature of advanced human carotid atherosclerosis assessed by mass spectrometry imaging, J. Lipid Res. 62 (2021), https://doi.org/10.1194/JLR.RA120000974.
[37] S. Iskander-Rizk, M. Visscher, A.M. Moerman, et al., Micro Spectroscopic Photoacoustic (μsPA) imaging of advanced carotid atherosclerosis, Photoacoustics 22 (2021), https://doi.org/10.1016/j.pacs.2021.100261.
[38] M. Visscher, A.M. Moerman, P.C. Burgers, et al., Data processing pipeline for lipid profiling of carotid atherosclerotic plaque with mass spectrometry imaging, J. Am. Soc. Mass Spectrom. 30 (9) (2019) 1790–1800, https://doi.org/10.1007/s13361-019-02254-y.
[39] J. Lim, J.T. Aguilan, R.S. Sellers, et al., Lipid mass spectrometry imaging and proteomic analysis of severe aortic stenosis, J. Mol. Histol. 51 (5) (2020) 559–571, https://doi.org/10.1007/s10735-020-09905-5.
[40] M. Martin-Lorenzo, B. Balluff, A.S. Maroto, et al., Molecular anatomy of ascending aorta in atherosclerosis by MS Imaging: specific lipid and protein patterns reflect pathology, J Proteomics 126 (2015) 245–251, https://doi.org/10.1016/j.jprot.2015.06.005.
[41] W. Li, J. Luo, F. Peng, et al., Spatial metabolomics identifies lipid profiles of human carotid atherosclerosis, Atherosclerosis 364 (2023) 20–28, https://doi.org/10.1016/j.atherosclerosis.2022.11.019.
[42] E.H. Seeley, Z. Liu, S. Yuan, et al., Spatially resolved metabolites in stable and unstable human atherosclerotic plaques identified by mass spectrometry imaging, Arterioscler. Thromb. Vasc. Biol. 43 (9) (2023) 1626–1635, https://doi.org/10.1161/ATVBAHA.122.318684.
[43] N.H. Patterson, R.J. Doonan, S.S. Daskalopoulou, et al., Three-dimensional imaging MS of lipids in atherosclerotic plaques: open-source methods for reconstruction and analysis, Proteomics 16 (11–12) (2016) 1642–1651, https://doi.org/10.1002/pmic.201500490.
[44] D. Kale, A. Fatangare, P. Phapale, A. Sickmann, Blood-derived lipid and metabolite biomarkers in cardiovascular research from clinical studies: a recent update, Cells 12 (24) (2023) 2796, https://doi.org/10.3390/cells12242796.
[45] C.V. Felton, D. Crook, M.J. Davies, M.F. Oliver, Relation of Plaque Lipid Composition and Morphology to the Stability of Human Aortic Plaques, vol. 17, 1997. http://ahajournals.org.
[46] E.A. Kaperonis, C.D. Liapis, J.D. Kakisis, D. Dimitroulis, V.G. Papavassiliou, Inflammation and atherosclerosis, Eur. J. Vasc. Endovasc. Surg. 31 (4) (2006) 386–393, https://doi.org/10.1016/j.ejvs.2005.11.001.
[47] L. Ménégaut, A. Jalil, C. Thomas, D. Masson, Macrophage fatty acid metabolism and atherosclerosis: the rise of PUFAs, Atherosclerosis 291 (2019) 52–61, https://doi.org/10.1016/j.atherosclerosis.2019.10.002.
[48] S. Lee, K.G. Birukov, C.E. Romanoski, J.R. Springstead, A.J. Lusis, J.A. Berliner, Role of phospholipid oxidation products in atherosclerosis, Circ. Res. 111 (6) (2012) 778–799, https://doi.org/10.1161/CIRCRESAHA.111.256859.
[49] H. Tanaka, N. Zaima, T. Sasaki, et al., Lysophosphatidylcholine acyltransferase-3 expression is associated with atherosclerosis progression, J. Vasc. Res. 54 (4) (2017) 200–208, https://doi.org/10.1159/000473879.
[50] Y. Matsuoka, M. Takahashi, Y. Sugiura, et al., Structural library and visualization of endogenously oxidized phosphatidylcholines using mass spectrometry-based techniques, Nat. Commun. 12 (1) (2021) 6339, https://doi.org/10.1038/s41467-021-26633-w.
[51] N. Slijkhuis, M. Towers, M. Mirzaian, et al., Identifying lipid traces of atherogenic mechanisms in human carotid plaque, Atherosclerosis 385 (2023) 117340, https://doi.org/10.1016/j.atherosclerosis.2023.117340.
[52] M.S. Boskamp, J. Soltwisch, Charge distribution between different classes of glycerophospolipids in MALDI-MS imaging, Anal. Chem. 92 (7) (2020) 5222–5230, https://doi.org/10.1021/acs.analchem.9b05761.
[53] F.B. Eiersbrock, J.M. Orthen, J. Soltwisch, Validation of MALDI-MS imaging data of selected membrane lipids in murine brain with and without laser postionization by quantitative nano-HPLC-MS using laser microdissection, Anal. Bioanal. Chem. 412 (25) (2020) 6875–6886, https://doi.org/10.1007/s00216-020-02818-y.
[54] J. Soltwisch, B. Heijs, A. Koch, S. Vens-Cappell, J. Höhndorf, K. Dreisewerd, MALDI-2 on a trapped ion mobility quadrupole time-of-flight instrument for rapid mass spectrometry imaging and ion mobility separation of complex lipid profiles, Anal. Chem. 92 (13) (2020) 8697–8703, https://doi.org/10.1021/acs.analchem.0c01747.
[55] M. Piccoli, F. Cirillo, A. Ghiroldi, et al., Sphingolipids and atherosclerosis: the dual role of ceramide and Sphingosine-1-phosphate, Antioxidants 12 (1) (2023) 143, https://doi.org/10.3390/antiox12010143.
[56] C. Bookmeyer, U. Röhling, K. Dreisewerd, J. Soltwisch, Single-photon-induced post-ionization to boost ion yields in MALDI mass spectrometry imaging, Angew. Chem. Int. Ed. 61 (34) (2022), https://doi.org/10.1002/anie.202202165.
[57] M. Niehaus, J. Soltwisch, M.E. Belov, K. Dreisewerd, Transmission-mode MALDI-2 mass spectrometry imaging of cells and tissues at subcellular resolution, Nat. Methods 16 (9) (2019) 925–931, https://doi.org/10.1038/s41592-019-0536-2.
[58] W.H. Müller, E. De Pauw, J. Far, C. Malherbe, G. Eppe, Imaging lipids in biological samples with surface-assisted laser desorption/ionization mass spectrometry: a concise review of the last decade, Prog. Lipid Res. 83 (2021) 101114, https://doi.org/10.1016/j.plipres.2021.101114.
[59] J. Soltwisch, H. Kettling, S. Vens-Cappell, M. Wiegelmann, J. Müthing, K. Dreisewerd, Mass spectrometry imaging with laser-induced postionization, Science (1979) 348 (6231) (2015) 211–215, https://doi.org/10.1126/science.aaa1051.
[60] J.A. Michael, S.M. Mutuku, B. Ucur, et al., Mass spectrometry imaging of lipids using MALDI coupled with plasma-based post-ionization on a trapped ion mobility mass spectrometer, Anal Chem. 94 (50) (2022) 17494–17503, https://doi.org/10.1021/acs.analchem.2c03745.
[61] C. Doppler, B. Messner, T. Mimler, et al., Noncanonical atherosclerosis as the driving force in tricuspid aortic valve associated aneurysms - a trace collection, J. Lipid Res. 64 (3) (2023), https://doi.org/10.1016/j.jlr.2023.100338.
[62] R.G. McDonald, D.A. Poulos, B. Woodall, et al., A MALDI mass spectrometry imaging sample preparation method for venous Thrombosis with initial lipid characterization of Lab-made and murine clots, J. Am. Soc. Mass Spectrom. 34 (9) (2023) 1879–1889, https://doi.org/10.1021/jasms.3c00079.
[63] B. Patel, A.N. Makaryus, Artificial intelligence advances in the World of cardiovascular imaging, Healthcare (Switzerland) 10 (1) (2022), https://doi.org/10.3390/healthcare10010154.